IEEE Access
Multidisciplinary | Rapid Review | Open Access Journal

Received April 2, 2019, accepted April 21, 2019, date of publication April 29, 2019, date of current version May 10, 2019.

Digital Object Identifier 10.1109/ACCESS.2019.2913989

Lowest-Technical-Merit Design Methodology of Hypersonic Cruise Vehicle

WENKAI WANG, ZHONGXI HOU, XIANZHONG GAO, AND LILI CHEN
College of Aerospace Science and Engineering, National University of Defense Technology, Changsha 410073, China
Corresponding author: Zhongxi Hou (hzx@nudt.edu.cn)

This work was supported by the National Natural Science Foundation of China under Grant 11602298.

ABSTRACT In the design of hypersonic cruise vehicles, great effort is demanded to improve the performances of subsystems, namely structure, aerodynamics, and propulsion. Herein, effort demanded to realize a subsystem performance is quantified by technical merit. To achieve a feasible design, excessive technical merit of any one subsystem should be avoided. Accordingly, a lowest-technical-merit (LTM) design methodology has been proposed in this work. By this methodology, the design problem could be interpreted into a parametric optimization. The solution to such an optimization corresponds to the highest feasibility. The methodology has been implemented on two cases: deriving a hydrocarbon-fueled long-range cruiser from Boeing X-51A, and a hydrogen-fueled LAPCAT scenario from PREPHA. The simulation results show that LTM could achieve optimal allocations while satisfying different payload/range performances. The design methodology could help to improve the feasibility of hypersonic cruise vehicles. Furthermore, it could also be used in the design of other systems.

INDEX TERMS Hypersonic cruise vehicle, design methodology, technical merit, feasibility/accessibility.

NOMENCLATURE

a	Structural parameter related to overall weight
b	Structural parameter related to payload
C	Constraint of subsystems
c_i	Growth coefficient in technical-merit function
E	Lift-drag ratio L/D
f	System performance driver
I_{sp}	Specific impulse, s
Ma	Mach number
R	Range, m
P_i	Performance of the i-th subsystem
P_0	System performance
p_i	Normalized performance of the i-th subsystem
μ_F	Fuel mass fraction
μ_P	Payload capacity
ν	Inclination factor
ω	Weight factor
ψ_i	Technical merit of the i-th subsystem
ψ_0	System-gross technical merit
Superscripts:	
$+$	Topmost level of a performance
$-$	Floor level of a performance
D	Demonstrated maximum of a performance
B	Performance of basic scenario

The associate editor coordinating the review of this manuscript and approving it for publication was Chaoyong Li.

I. INTRODUCTION

Hypersonic cruise vehicle (HCV) is a kind of vehicle that flies at speed beyond Ma 5. It mainly works in a cruising mode. The advantage of HCV is a combination of high speed and high efficiency. Because of the high speed, hypersonic vehicles could deliver payloads faster than subsonic/supersonic airplanes does. This ability makes hypersonic airliners, such as LAPCAT-II [1] and HEXAFLY-Int [2], [3], a research hotspot. ISR, strike, or other national need missions have stimulated the requirement for high speed operational systems, e.g. Falcon Blackswift/HTV-3X [4].

Although rockets are also suitable for high-speed flights, airbreathing engines such as ramjets or scramjets could absorb oxygen from the atmosphere, thus leading to less mass consumption during combustion to achieve a given thrust. With the airbreathing engines adopted, HCV could achieve higher specific impulses or propulsive efficiencies [5]. Therefore, HCV is more promising to realize a long-range high-speed flight. Besides, since rocket is inefficient at low speed, HCV also makes a better candidate for launch vehicle

in multi-stage-to-orbit missions [6], for example, Sänger Spaceplane [7].

Therefore, the prompt/efficient advantage of HCV is significant in the applications. Nevertheless, the long-range high-speed flight in atmosphere challenges nearly all the subsystems in design of HCV. For each of the subsystems, there are considerable technical problems to overcome. Due to these problems, a prospective/applicable performance is difficult to realize.

Specific impulse is a description of propulsive performance. It is related to the thermal cycle of engine and flight conditions of vehicle. However, the high-speed internal flow proposes problems in unstart of inlet [8]–[10], combustion stabilization [11], and thermal protection [12], [13]. Because of these problems, propulsive performance of HCV is difficult to realize and improve [14]. To solve these problems, techniques such as waverider forebodies [15], novel configurations of inlets/diffusers (for example, Busemann inlet [16] and Lens Analogy inlet/diffuser [17], [18]), precooling [19], recycling of energy [20], and active control (for example, control system with a combination of Wheeler Doublets and vortex generator jets [21]) have become research focuses. However, adoption of these techniques would also introduce new problems, for example, higher empty weight caused by additional components.

L/D (lift-to-drag ratio) is a description of aerodynamic performance. Because of the strong compression at shock waves and the high viscous effect, high drag would be yielded on a hypersonic vehicle [22]. This is the reason for the decline of theoretical aerodynamic performance. To improve the aerodynamic performance, waverider [23], [24], counterflowing aerospike/aerodisk [25]–[27], high-slenderness configurations [27], [28] have been proven effective. However, the aerodynamic performance of waverider is difficult to maintain when engine and control panels are integrated [29], [30]. The technique of counterflowing aerospike/aerodisk demands aerospike/aerodisk and workflow, whereas that of slender configurations require stronger structure. Hence the two techniques would lead to higher empty ratio.

Besides, a sharp leading edge is also preferable for aerodynamic performance [31]. However, speed beyond Mach 5 would induce prominent aerodynamic heating on surfaces [32]. The heat flux at the leading edge is in negative correlation with the local radius of curvature. That means a trade-off of bluntness is demanded [33]. Hence thermal protection would put forward a restriction for aerodynamic performance. Moreover, to endure the long-time aerodynamic heating, a comprehensive thermal protection system (TPS) consists of passive, radiative, and active cooling techniques is demanded [34], [35]. This would lead to a higher empty ratio [36].

Therefore, long-range hypersonic cruise challenges aerodynamics and propulsion performances. The techniques to improve the two performances would probably introduce new problems in design, especially a high empty ratio. A high empty ratio means a poor structural performance or a low useful fraction (including fuel and payload). From the perspective of Breguet's range formula, range is in positive correlations with specific impulse, L/D, and fuel capacity. To realize a given range, low propulsive and aerodynamic performances would lead to a high requirement for fuel capacity. Hence the payload capacity of HCV is limited. For a given range, payload capacity could evaluate the integral performance involving propulsion, aerodynamics, and structure. According the review above, the performances of the three subsystems are restrained by bundles of technical problems. Then a higher performance means less feasibility and more technical effort. In a design of a HCV pursuing a high payload capacity or a long range, the feasibility/accessibility of the subsystem performances should also be concerned.

To evaluate the feasibility/accessibility of a subsystem performance, technical merit is defined as a measure of technical effort to make. Technical merit is in negative correlation with feasibility/accessibility, whereas in positive one with performance. For a certain subsystem, a high performance would demands more advanced techniques or breakthroughs, thus leading to more technical merit but low feasibility/accessibility. A weighted combination of the technical merits of the involved subsystems could provide a comprehensive consideration of the system-gross technical merit. For a scenario with the lowest system-gross technical merit, to reduce the technical merit of a certain subsystem, the others need to be paid with more. Hence the lowest technical merit is a point where a balance or compromise exists among the subsystems. To obtain such a scenario, the problem could be formulated as a parametric optimization to minimize the system-gross technical merit, or a multi-objective one to minimize the technical merits of all the subsystems. Accordingly, a lowest-technical-merit (LTM) design methodology is proposed herein.

The design problem of hypersonic cruise vehicle is formulated as one to satisfy the payload/range performance. According to the performance driver, subsystems include structure, aerodynamics, and propulsion. The topmost, floor, and demonstrated levels of the subsystems have been made clear by statistics, on the basis of current theories and technologies. The methodology has been implemented on two cases: deriving a hydrocarbon-fueled long-range cruiser from Boeing X-51A, and a hydrogen-fueled LAPCAT scenario from PREPHA. In the two cases, LTM has proven effective to allocate the performances/improvement. Principal subsystems at different payload/ranges have been figured out.

II. LOWEST-TECHNICAL-MERIT DESIGN METHODOLOGY

A. DILEMMA IN DESIGN OF A SYSTEM

In design of a system, the basic organization consists of upstream, system designer, and subsystems, as shown in Fig. 1. The upstream proposes the system performance P_0 of the whole system to be maximized. This role could be played by customer or system designer of upper level.

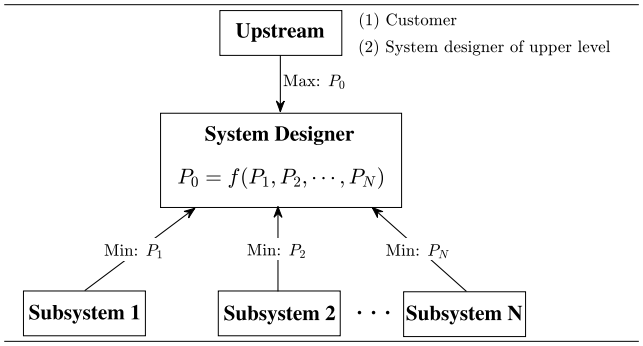

FIGURE 1. Sketch map of a system design.

The system designer has the duty to realize the system performance by joint efforts of the subsystems. However, from the perspective of a certain subsystem designer, improvement of the performance P_i ($i \in [1, N]$) is related to advances of technology. This would lead to additional technical effort to realize and technical difficulties to implement. Hence the performance allocated to each of the subsystems is desired to be minimized. From the perspective of the system designer, there are two problems in concern:

(1) the system performance P_0 should be satisfied at least and maximized at best;

(2) the performance of any one subsystem should not be too demanded, to avoid infeasibility caused by excessive technical effort and risks.

This leads to a dilemma to face for the system designer.

To deal with this dilemma, a lowest-technical-merit design methodology is proposed herein.

B. TECHNICAL MERIT

For a subsystem, its performance P_i could access a level no lower than the floor level P_i^-, whereas could not access the theoretical topmost P_i^+.

With the two boundaries involved, the performance could be normalized as (1). The equation indicates that p_i is a dimensionless quantity within 0-1. A normalized performance of 0 is related to the floor level P_i^-, whereas one of 1 is related to the topmost level P_i^+.

$$p_i = \frac{P_i - P_i^-}{P_i^+ - P_i^-} \in [0, 1) \tag{1}$$

For a subsystem, it is more difficult to adopt a higher normalized performance p_i, which means less feasibility/accessibility. The topmost, floor, demonstrated (maximum), and basic levels of subsystems of a design could be organized by Table. 1. In the table, P_i^+ is the theoretical topmost level, P_i^- is the floor level (minimum demonstrated level at present), P_i^D is the maximum demonstrated level at present, and P_i^B is the performance of the basic scenario.

To quantify the effort to achieve a subsystem performance, a technical merit is defined as a function of normalized performance, as shown in (2).

TABLE 1. The topmost/floor/demonstrated/basic levels of subsystems.

Subsystem No.	Topmost	Floor	Demonstrated	Basic
1	P_1^+	P_1^-	P_1^D	P_1^B
2	P_2^+	P_2^-	P_2^D	P_2^B
⋮	⋮	⋮	⋮	⋮
N	P_N^+	P_N^-	P_N^D	P_N^B

$$\psi_i = \Psi(p_i) \tag{2}$$

The technical-merit function Ψ should satisfy the following properties:

(1) Technical merit is in positive correlation with normalized performance. Hence it is monotone increasing, as shown in (3).

$$\Psi_i' = \frac{\mathrm{d}\Psi_i}{\mathrm{d}p_i} > 0 \tag{3}$$

(2) Improvement on the basis of a higher performance would be more difficult. Hence the second derivative of technical merit is positive, as shown in (4).

$$\Psi_i'' = \frac{\mathrm{d}^2\Psi_i}{\mathrm{d}p_i^2} > 0 \tag{4}$$

(3) Technical merit is a relative quantity whose single value is without physical significance. The base point is related to the floor performance. The technical merit at the floor level could be set to 0, as shown in (5).

$$\Psi_i(0) = 0 \tag{5}$$

(4) The development of theory is in advance of realization. Hence the topmost level is inaccessible at current technology level, which lies an asymptotic line for technical merit, as shown in (6).

$$\lim_{p_i \to 1} \Psi_i(p_i) \to +\infty \tag{6}$$

(5) Since technical merit is a relative quantity, two technical-merit functions in linear correlations, Ψ_i and $\tilde{\Psi}_i$ shown in (7), are equivalent. c is a constant.

$$\tilde{\Psi}_i = c\Psi_i, \quad (c > 0) \tag{7}$$

According to the last property, if a technical-merit function crosses Point (0.5, 1), as shown in (8), it could be called as basis function. This definition means that for a normalized performance p_i of 0.5, the technical merit of the subsystem is 1. A basis function is adequate to describe the correlation between technical merit and normalized performance of one subsystem.

$$\Psi(0.5) = 1 \tag{8}$$

Here gives several alternative basis functions Ψ. The curves of the functions are plotted in Fig. 2. The figure indicates that the function in (11) with coefficient $c_i = 0.5$ could

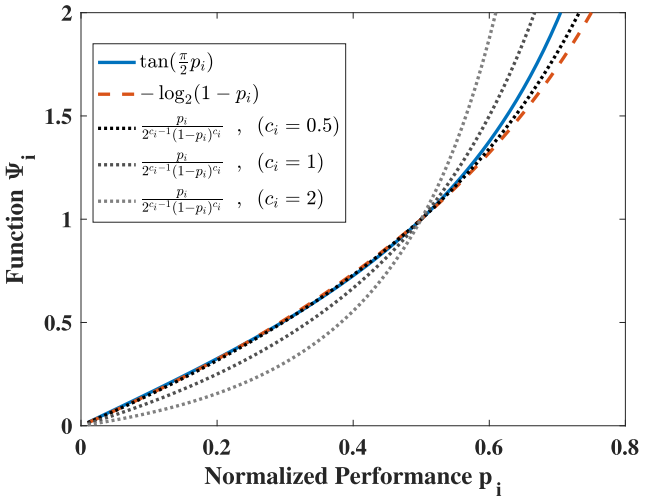

FIGURE 2. Curves of alternative basis functions Ψ.

approximate that in (9) and (10). Therefore, only (11) is adopted to estimate the technical merits of the subsystems. The subsystems are different in the coefficient c_i. Fig. 2 also indicates that a higher c_i yields a lower technical merit at $p_i < 0.5$ whereas a higher at $p_i > 0.5$. Hence c_i is in positive correlation with Ψ''. A higher c_i means the growth ratio of technical merit along with normalized performance would increase faster. Accordingly, c_i is called as growth coefficient herein.

$$\Psi_i = \tan\left(\frac{\pi}{2}p_i\right) \tag{9}$$

$$\Psi_i = -\log_2(1-p_i) \tag{10}$$

$$\Psi_i = \frac{p_i}{2^{c_i-1}(1-p_i)^{c_i}}, \quad (c_i > 0) \tag{11}$$

For a design with a basic scenario, the technical merit of a subsystem should base on that of the scenario, as shown in (12).

$$\psi_i = \Psi(p_i) - \Psi\left(p_i^B\right) \tag{12}$$

C. SYSTEM-GROSS TECHNICAL MERIT

To include impacts of subsystems on the system, technical merits could be multiplied by weight factors. Weight factor is a property of a subsystem. Accordingly, the system-gross technical merit could be estimated by a weighted sum of the technical merits of all its subsystems, as shown in (11).

$$\psi_0 = \sum_{i=1}^{N} \omega_i \psi_i, \quad \left(\omega_i \geq 0, \ \sum_{i=1}^{N} \omega_i = 1\right) \tag{13}$$

ω_i is the weight factor of the i-th subsystem. A higher weight factor ω_i means more contribution of the subsystem to the system-gross technical merit. In minimization of the latter, the performance of the subsystem would be less demanded, which is desirable for the subsystem. Therefore, each subsystems tends to conceive a high weight factor, which causes a trade-off among the subsystems. That means the weight factor of each subsystem should be accepted by all the subsystems. Accordingly, a strategy to conduct such a trade-off is demanded. To realize such a trade-off, the system designer needs to coordinate the opinions of the subsystems. Herein, two optional strategies are offered:

TABLE 2. Weight factors of subsystems.

Subsystem No.	1	2	$\cdots$	N	Sum
1	$\omega_1^{(1)}$	$\omega_2^{(1)}$	$\cdots$	$\omega_N^{(1)}$	1
2	$\omega_1^{(2)}$	$\omega_2^{(2)}$	$\cdots$	$\omega_N^{(2)}$	1
$\vdots$	$\vdots$	$\vdots$	$\ddots$	$\vdots$	$\vdots$
N	$\omega_1^{(N)}$	$\omega_2^{(N)}$	$\cdots$	$\omega_N^{(N)}$	1
Average	ω_1	ω_2	$\cdots$	ω_N	1

(1) Subjective strategy. All the subsystems put forward weight factors to each other; and the weight factor of one subsystem is the average of all that it received, as shown in Table. 2. $\omega_i^{(j)}$, $(i, j \in [1, N])$ denotes the weight factor put forward by the j-th subsystem to the i-th one. This strategy could also be formulated as

$$\begin{cases} \omega_i = \dfrac{1}{N}\sum\limits_{j=1}^{N} \omega_i^{(j)}, & (\forall i \in [1, N]) \\ \sum\limits_{i=1}^{N} \omega_i^{(j)} = 1, & (\forall j \in [1, N]) \end{cases} \tag{14}$$

(2) Objective strategy. All the subsystems acknowledge that the technical merits ($\omega_i\psi_i$) corresponds to their P_i^D are the same. Since weight factor is an objective knowledge on how much a subsystem contributes to the system-gross technical merit, it should be independent on basic scenarios. Then $\omega_i\Psi_i$ of all the subsystems should also be equal. The strategy could be formulated as

$$\begin{cases} \omega_1\Psi_1\left(p_1^D\right) = \omega_2\Psi_2\left(p_2^D\right) = \cdots = \omega_N\Psi_N\left(p_N^D\right) \\ \sum\limits_{i=1}^{N} \omega_i = 1 \end{cases} \tag{15}$$

If development of a subsystem is to stimulate, a high performance of this subsystem should be permitted in minimization of the system-gross technical merit. With the system-gross technical merit in (13) recognized as performance measure of a multi-objective optimization, the weight factor of this subsystem should decrease. With the subjective inclination level quantized by ν_i, the system-gross technical merit could be revised as (16).

$$\psi_0 = \sum_{i=1}^{N} \nu_i \omega_i \psi_i, \quad (0 < \nu_i \leq 1) \tag{16}$$

$\nu_i \in (0, 1]$ is the inclination factor of the i-th subsystem. Its default value is 1. When no subjective inclination is considered, the default should be adopted. If development of the i-th subsystem is to stimulate, a $\nu_i < 1$ should be adopted. In some circumstances, for example, the capacity/potential of the i-th

TABLE 3. Composition of system-gross technical merit.

Subsystem No.	Growth	Weight	Inclination
1	c_1	ω_1	ν_1
2	c_2	ω_2	ν_2
⋮	⋮	⋮	⋮
N	c_N	ω_N	ν_N

subsystem designer is limited, the performance/improvement of this subsystem should be restrained. Then a $\nu_i > 1$ should be adopted.

Therefore, the system-gross technical merit contributed by each subsystem consists of three parts:

(1) Ψ_i (or c_i) describing the growth of technical merit along with subsystem performance, decided by each subsystem;
(2) ω_i describing the contribution of each subsystem, accepted by all the subsystems;
(3) ν_i describing the subjective inclination level to each subsystem, proposed by the system designer.

Accordingly, the terms of system-gross technical merit could be organized by Table. 3

D. LOWEST-TECHNICAL-MERIT DESIGN METHOD

The design problem of a system could be formulated into a parametric optimization as follows:

$$\begin{aligned} &\text{Find} : P_1, P_2, \cdots, P_N \\ &\text{Min} : \psi_0 \\ &\text{Satisfy} : f(P_1, P_2, \cdots, P_N) \geq P_0 \\ &\text{s.t.} \begin{cases} P_i \in [P_i^-, P_i^+] \quad i = 1, 2, \cdots, N \\ C(P_1, P_2, \cdots, P_N) \leq 0 \end{cases} \end{aligned} \tag{17}$$

where, f is the system performance driver. C is the inequality constraint include couplings among the performances of subsystems. This formulation means to find a set of physically significant performances, with system performance and constraints satisfied, and with the system-gross technical merit minimized. Hence this methodology is called as lowest-technical-merit (LTM) design methodology. Reducing technical merit in one subsystem would lead to more technical merit increment in the others. The optimization could also be recognize as a multi-objective one to minimize the technical merits of all the subsystems. Then an excessive subsystem performance could be avoided. Therefore, the LTM design methodology could provide a balance allocation of performances among the subsystems.

A LTM design could be implemented by steps shown in Fig. 3. The system performance driver should be firstly put forward. Accordingly, the involved subsystems could be listed. Then the topmost, floor, and demonstrated levels of each subsystem should be determined, on the basis of currently theories and technologies. The technical-merit function of each subsystem should be specified according to the growing feature of technical effort. The weight factor

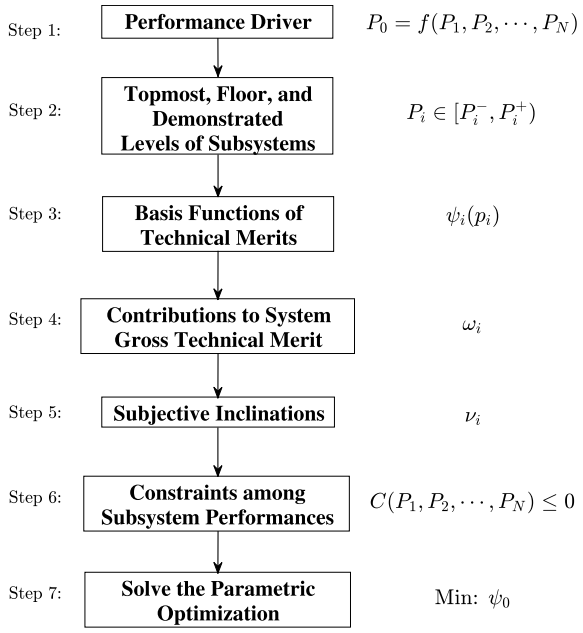

FIGURE 3. Steps of the Lowest-Technical-Merit design methodology.

of each subsystem should be estimated on the basis of the demonstrated level. The inclination factor should be provided by the system designer to decide which subsystem is to stimulate. Afterwards, the constraints among the subsystems should also be modeled. Then the design problem could be interpreted into a parameter optimization to minimize the system-gross technical merit. By solving the optimization problem, the subsystem performances could be determined.

Technical merit provides a way to compare the performances of different subsystems. The subsystem with the highest technical merit ($\omega_i\psi_i$) should be assigned with the highest performance or improvement. Such a subsystem is called as the principal subsystem.

E. RECURSION OF METHODOLOGY

The tree map of a multi-level system is shown in Fig. 4. According to the figure, design of each subsystem could also be recognized as an independent problem. With LTM implemented on the i-th subsystem, its technical merit is the weighted sum of that of its secondary subsystems. The technical-merit function Ψ_i could be obtained by

$$\begin{cases} \Psi_i = \dfrac{\sum_{j=1}^{N_i} \omega_{ij}\psi_{ij}(p_{ij})}{\sum_{j=1}^{N_i} \omega_{ij}\psi_{ij}(0.5)} \\ p_i = f_i(p_{i1}, p_{i2}, \cdots, p_{iN_i}) \end{cases} \tag{18}$$

where, N_i is the number of secondary subsystems of the i-th subsystem. ω_{ij}, ψ_{ij}, and p_{ij} are respectively weight factor, technical merit, and normalized performance of the j-th

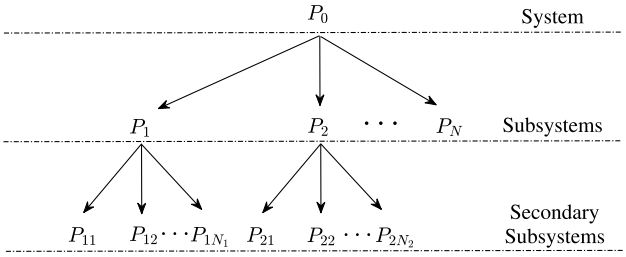

FIGURE 4. Dendrogram.

secondary subsystem. f_i is the performance driver of the i-th subsystem. On the basis of the $\Psi_i - p_i$ curve of (18), growth coefficient of the i-th subsystem could be obtained by fitting. The fitted curve should approximate (18) especially within $p_i \in [p_i^B, 1)$.

Besides, for a subsystem contains no secondary subsystems, the technical-merit function in (11) with a growth coefficient of 0.5 could be adopted.

III. DESIGN PROBLEM OF A HYPERSONIC CRUISE VEHICLE

A. SYSTEM PERFORMANCE DRIVERS: PAYLOAD/RANGE

Küchemann has provided a weight breakdown analysis, as shown in (19). a and b are structural parameters. a involves components whose weight is proportional to the overall weight, including wings, undercarriage, services and equipments. b involves components whose weight is proportional to payload, including fuselage, furnishings and the payload itself.

$$W = aW + bW_P + W_F + W_E \tag{19}$$

W_E is the weight of engine. In a HCV, the mass and the thrust of scramjets/ramjets are proportional to the cowl area A, as shown in (20) and (21). I_E is the areal density of engine, q is the dynamic pressure, C_T is the thrust coefficient.

$$W_E = I_E A g \tag{20}$$

$$T = qAC_T \tag{21}$$

Besides, the thrust is also proportional to the gross weight of vehicle, as shown in (22). (T/W) is the thrust-weight ratio. It is a design index related to acceleration and maneuverability.

$$T = (T/W) \cdot W \tag{22}$$

With (20)-(22) combined, the weight of engine could be revised as (23). It is proportional to gross weight of vehicle.

$$W_E = \frac{I_E g}{qC_T}(T/W) \cdot W \propto W \tag{23}$$

With (23) substituted into (19), W_E could be contained in the function term aW. Then the gross weight could be revised as

$$W = aW + bW_P + W_F \tag{24}$$

With two sides of (24) divided by gross weight, the payload capacity of the HCV could be estimated by

$$\mu_P = \frac{1}{b}(1 - \mu_F - a) \tag{25}$$

μ_F is the fuel mass fraction consumed over the cruising process. It could be estimated by Breguet's range formula, as shown in (26). The estimation is derived from a steady cruise with constant velocity and constant L/D.

$$\begin{aligned} R &= -VI_{sp}E \cdot \ln(1 - \mu_F) \\ \Rightarrow \mu_F &= 1 - \exp\left(-\frac{R}{VI_{sp}E}\right) \end{aligned} \tag{26}$$

With (26) substituted into (25), the latter could be revised as (27). a and b are related to structural performance; I_{sp} is propulsive performance; E is aerodynamic performance. Besides, R is range, V is velocity. The equation indicates that a long range could lead to a low payload capacity. Hence range and payload are a couple of contradictories. With one of them specified, by (27), the other could make the performance evaluation of hypersonic cruise vehicles. Accordingly, the system performance is described by a couple of payload/range.

$$\mu_P = \frac{1}{b}\left[\exp\left(-\frac{R}{VI_{sp}E}\right) - a\right] \tag{27}$$

In such a performance driver, three subsystems are involved in the performance driver, namely structure, aerodynamics, and propulsion.

B. SUBSYSTEM 1: STRUCTURE

a and b are in negative correlation with structural performance. Smaller a and b mean higher structural efficiency. Steelant's statistics [37] indicates that a ranges within 0.2-0.4, whereas that b ranges within 1.75-2.25. Accordingly, a could be considered as the principal factor of structural performance, whereas $b = 2$ is adopted. Hence the structural performance could be formulated as

$$P_1 = -a \tag{28}$$

For an existing vehicle, the structural performance could be estimated by its payload and fuel capacities, as shown in (29).

$$P_1 = \mu_F + b\mu_P - 1 \tag{29}$$

Payload and fuel capacities of supersonic/hypersonic vehicles are plotted in Fig. 5. The data shown in the figure consist of following parts:

(1) LAPCAT concepts [37]–[39]: MR2.4/M4.5/M8/A2 scenarios.

(2) Other hypersonic concepts: HyperSoar 2000 [40], [41], NASP X30 [42], NASA Ma6 Transport/Fighter [43], and recalculated Scale 1 PREPHA Vehicle [38].

(3) Demonstrated Hypersonic Vehicles: Lockheed HYCAT-1/1A/4 [43], ROCKWELL Vehicle [43], X-15 [37], and X-51A [44].

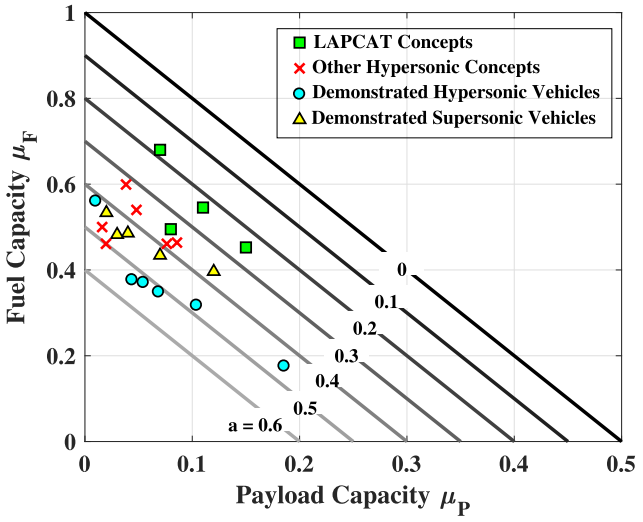

FIGURE 5. Fuel/payload capacities and structural performances of high-speed vehicles.

(4) Demonstrated Supersonic Vehicles [37]: Tu-144D, Concorde, XB-70A, Sukhoi T-4, SR-71.

The levels of a are also shown in Fig. 5. The figure indicates that the structural performance of demonstrated hypersonic vehicles are located within $[-0.6, -0.4]$. That of hypersonic concepts (including LAPCAT scenarios) are higher, because of the improvement of structure technology. That of the demonstrated supersonic vehicles are also higher than that of the demonstrated hypersonic ones, because of the thermal protection system adopted in the latter.

C. SUBSYSTEM 2: AERODYNAMICS

The aerodynamic performances have been attained by hypersonic vehicles are shown in Fig. 6. Wherein, the data of models including CAV, Sänger Spaceplane, X-34, and X-38 are from Ernst's book [7], that of X-33 is from Murphy's work [45], that of Boeing X-51A is from Mutzman's [46], and that of X-43A is from Engelund's [47]. Besides, data in works namely Williams [48], Harloff [49], Feng *et al.* [50], Lewis [30], Wang *et al.* [51], and Huiyu *et al.* [52] are also referred.

In this figure, aerodynamic performances at different Mach numbers could be divided into three regions:

(1) From 1 to 3.5: demonstrated vehicles locate.

(2) From 3.5 to E_C: most numerical simulations and aerodynamic experiments of clean configurations locate. E_C is defined in (30).

$$E_C = \frac{4(Ma+3)}{Ma} \tag{30}$$

(3) From E_C to E_B: most theoretical estimations/predictions locate. E_B is the L/D barrier defined in (31).

$$E_B = \frac{6(Ma+2)}{Ma} \tag{31}$$

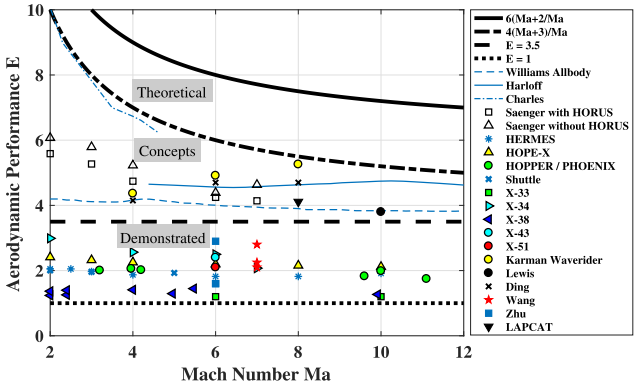

FIGURE 6. Aerodynamic performances of different hypersonic vehicles.

According to the figure, $E_D = 3.5$ could be adopted. The difference between E_D and E_B is caused by bluntness, and integration of control surfaces and propulsion system. According to Wang's work [51], these factors could cause decline of aerodynamic performance by more than 50%. The similar conclusions have also been obtained by Lewis [30] and Charles *et al.* [29].

According to the figure, at present, E_B is still the theoretical topmost level of aerodynamic performance; L/D of 1 could be recognized as the floor.

D. SUBSYSTEM 3: PROPULSION

Specific impulse is a performance of propulsion system. It describes the available thrust per fuel mass flowrate, as shown in (32). To satisfy a given thrust requirement, a propulsion system with higher specific impulse would consumes less fuel.

$$I_{sp} = \frac{T}{\dot{m}_F g} \tag{32}$$

According to Heiser and Pratt [53], specific impulse of ramjets/scramjets could be estimated by

$$I_{sp} = \frac{V}{fg}\left[-1 + \sqrt{\eta_{KE}(1+f)\left(1 + \frac{\eta_b f h_{PR}}{h_{t0}}\right)}\right] \tag{33}$$

where, η_{KE} is kinetic efficiency; h_{t0} is the specific total enthalpy, as shown in (34).

$$h_{t0} = c_p T_0 + \frac{1}{2}V_0^2 = c_p T_0\left(1 + \frac{\gamma-1}{2}Ma^2\right) \tag{34}$$

With a static temperature of $T_0 = 250$ K adopted, this estimation is independent on altitude. With an $\eta_{KE} = 1$ adopted, the result is the topmost level of propulsive performance in theoretical.

Kuranov *et al.* [54] has provided a statistics about specific impulse of different airbreathing engines. The current available performances of ramjets, scramjets, and rockets are shown in Fig. 7. Data of X-51A and SABRE are also plotted.

The maximum available specific impulse of rockets could be adopted as the floor level of hydrocarbon-fueled

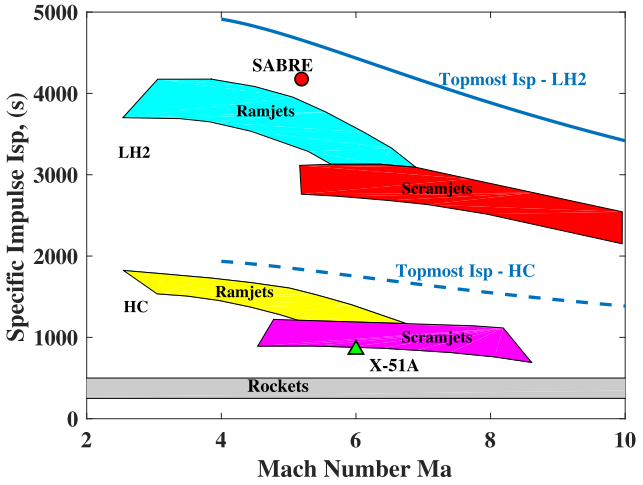

FIGURE 7. Propulsive performances of demonstrated ramjets/scramjets.

airbreathing engines, whereas that the topmost level of hydrocarbon ones could be adopted as that of hydrogen-fueled ones.

IV. LTM DESIGN OF HYPERSONIC CRUISE VEHICLES

A. INTERPRETATION OF LTM DESIGN PROBLEM

To allocate the improvements to achieve a most feasible scenario, LTM is implemented. A hypersonic cruise vehicle with the subsystem performances resulted from LTM design is called as LTM-HCV herein.

The design problem could be interpreted into a parametric optimization, as shown in (35).

$$\begin{aligned} &\text{Find}: P_1, E, I_{sp} \\ &\text{Min}: \psi_0 \\ &\text{Satisfy}: \frac{1}{b}\left[\exp\left(-\frac{R}{VI_{sp}E}\right)+P_1\right] \geq \mu_P \\ &\text{s.t.} \begin{cases} P_1 \in [P_1^-, P_1^+] \\ E \in [E^-, E^+] \\ I_{sp} \in [I_{sp}^-, I_{sp}^+] \end{cases} \end{aligned} \tag{35}$$

B. CASE 1: FROM X-51A TO A LONG-RANGE CRUISER

X-51A has demonstrated technologies of structure (light materials/structure), aerodynamics (waverider), and propulsion (scramjet). As a demonstrator, it is unnecessary to possesses a long range or a high payload capacity. Specifications of Boeing X-51A are shown in Table. 4. The table indicates that range of X-51A is only 740 km. To derive a long-range cruiser from X-51A, the three subsystems should be improved. LTM is implemented to allocate the improvements, with X-51A adopted as the basic scenario. The specifications of the cruiser are also shown in Table. 4. As X-51A does, the cruiser adopts JP-7 fuel, and flies at Ma 6.

The topmost/floor/demonstrated/basic levels of each subsystem are specified in Table. 5. It should be noted that the topmost of aerodynamics, and the topmost and demonstrated

TABLE 4. Specifications of boeing X-51A and long-range cruiser.

Parameter	Fuel	Ma	R	μ_P
Unit	-	-	10^3 km	–
Boeing X-51A	JP-7	6.0	0.74	0.1855
Long-range cruiser	JP-7	6.0	4-12	0.1

TABLE 5. The topmost/floor/demonstrated/basic levels of subsystems of the long-range cruiser.

Subsystem No.	Topmost	Floor	Demonstrated	Basic
1 - Structure	0	-0.4	-0.6	-0.45
2 - Aerodynamics	8	3.5	1	2.5
3 - Propulsion	1750	1380	500	850

TABLE 6. Composition of system-gross technical merit of the long-range cruiser.

Subsystem No.	Growth	Weight	Inclination
1 - Structure	0.5	0.4432	1
2 - Aerodynamics	0.5	0.4062	1
3 - Propulsion	0.5	0.1506	1

of propulsion are relative with Mach number. The levels of propulsion are also dependent on the fuel type, JP-7.

The components of system-gross technical merit are shown in Table. 6 The growth coefficients of the subsystems are set as 0.5. The weight factors are estimated by the strategy in (15) and the levels in Table. 5. Table. 6 indicates that propulsion possesses the lowest weight factor, followed by aerodynamics. The inclination factors of the subsystems are set as 1, i.e. there is no subjective inclination among the subsystems.

Design results of the cruiser with different ranges are shown in Fig. 8. The figure indicates that the technical merits and performances of the subsystems increase with range. The technical merits of the subsystems are plotted in Fig. 8.(a). Among the subsystems, when range is shorter than 7.8×10^3 km, aerodynamics is the principal subsystem where most technical merit should be paid. When range is longer than 7.8×10^3 km, structure becomes the principal. The performances of structure, aerodynamics, and propulsion are respectively plotted in Fig.8.(b), (c), and (d). For a range longer than 4×10^3 km, the aerodynamic performance exceeds its demonstrated maximum; for one longer than 4.2×10^3 km, the structural does; for one longer than 10×10^3 km, the propulsive does. Therefore, advanced technologies of aerodynamics and structure are urgently desired to break through the currently demonstrated levels. This conclusion is in line with the published conceptual scenarios in Figs. 5,6, and 7.

C. CASE 2: FROM PREPHA TO A LAPCAT SCENARIO

LAPCAT II [38] is aimed to design a hypersonic airliner with a payload capacity of 60×10^3 kg and a range of 18.7×10^3 km. Re-evaluation of PREPHA [1], [38] at Ma 8 shows only adequate for a range of 13.5×10^3 km. To converge a LAPCAT scenario on the basis of PREPHA, the range

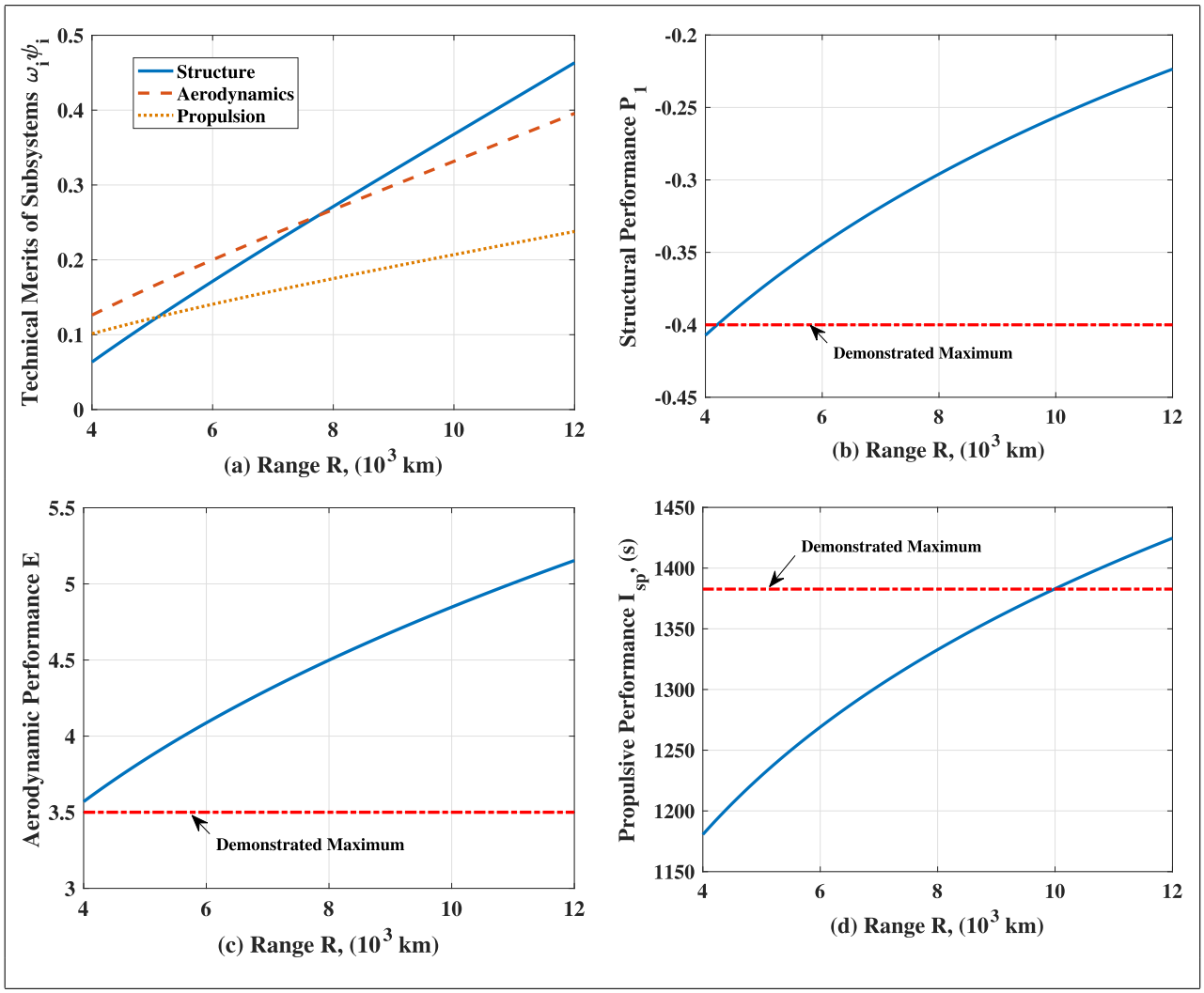

FIGURE 8. Long-range cruisers with different ranges. ($\mu_P = 0.1$).

TABLE 7. Specifications of PREPHA and LAPCAT scenarios.

Parameter	Fuel	Ma	R	μ_P	m_P
Unit	-	-	10^3 km	–	kg
PREPHA	LH2	8.0	13.6	0.0857	60×10^3
LAPCAT	LH2	8.0	18.7	0.05-0.3	60×10^3

TABLE 8. The topmost/floor/demonstrated/basic levels of subsystems of LAPCAT.

Subsystem No.	Topmost	Floor	Demonstrated	Basic
1 - Structure	0	-0.4	-0.6	-0.35
2 - Aerodynamics	7.5	3.5	1	3.42
3 - Propulsion	3885	3280	1550	2200

performance should be satisfied. Besides, the gross weight of the vehicle is also desired to reduce, which means a high payload capacity is pursued. LTM is implemented to realize such a design, with PREPHA adopted as the basic scenario. The specifications of the PREPHA and LAPCAT scenarios are shown in Table. 7. The two scenarios adopt liquid hydrogen as fuel. Besides, it should be noted that the payload capacity of PREPHA is estimated on the basis of payload weight 60 t and the gross weight 700 t.

The topmost/floor/demonstrated/basic levels of each subsystem are specified in Table. 8. The topmost of aerodynamics, and the topmost and demonstrated of propulsion are relative with Mach number. The levels of propulsion are also dependent on the fuel type, liquid hydrogen. The basic aerodynamic and propulsive performances are provided by re-evaluation of PREPHA, whereas the basic structural one is estimated on the basis of range. The table indicates that the structural performance of PREPHA exceeds the demonstrated. Since the former has not been demonstrated, it is only used as the basic; however, the demonstrated level maintains -0.4.

The components of system-gross technical merit are shown in Table. 9 The growth coefficients of the subsystems are set as 0.5. The weight factors are estimated by the strategy in (15)

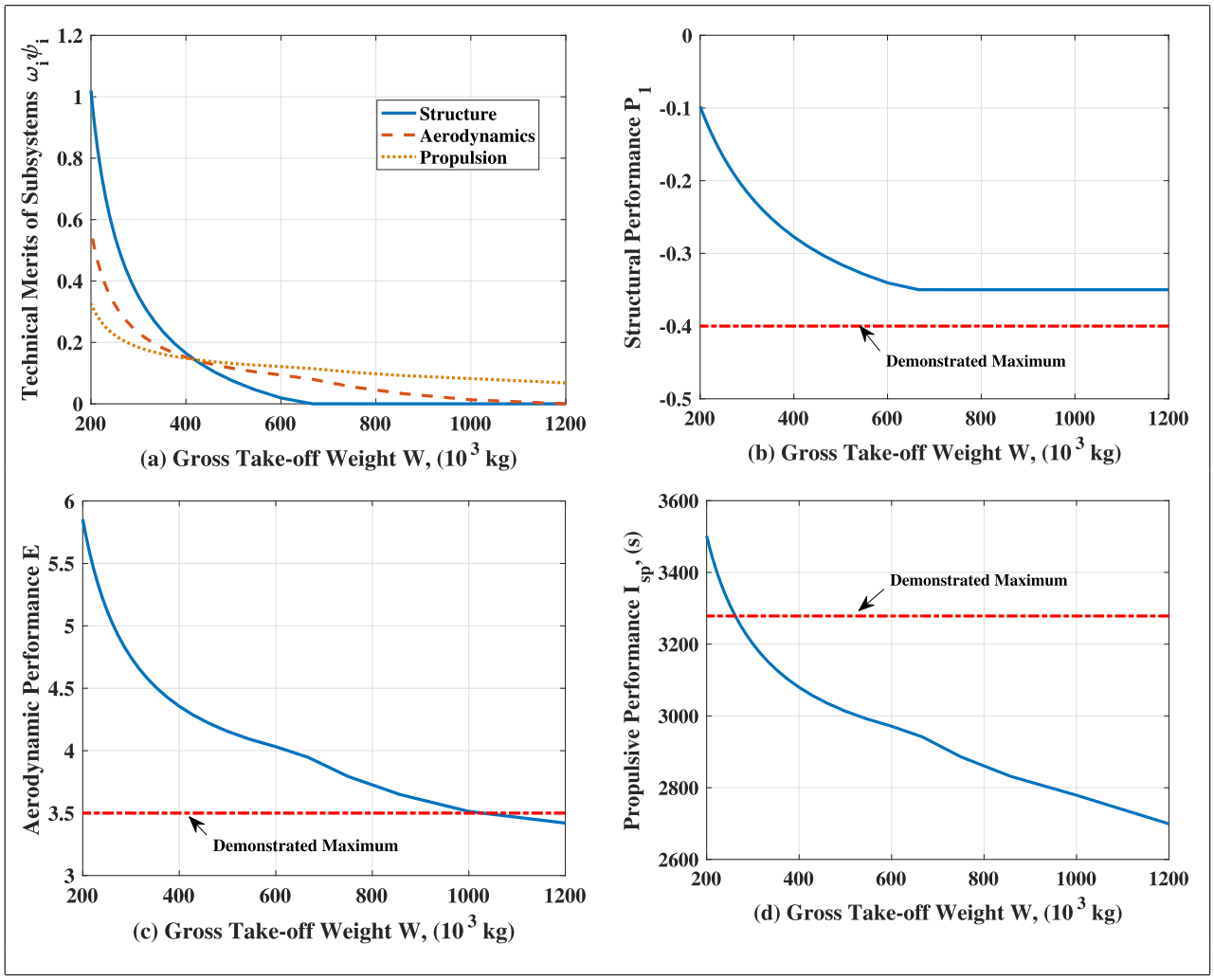

FIGURE 9. LAPCAT scenarios with different gross take-off weights.

TABLE 9. Composition of system-gross technical merit of LAPCAT.

Subsystem No.	Growth	Weight	Inclination
1 - Structure	0.5	0.4019	1
2 - Aerodynamics	0.5	0.4472	1
3 - Propulsion	0.5	0.1509	1

and the levels in Table. 8. Table. 9 indicates that propulsion possesses the lowest weight factor, followed by structure. The inclination factors of the subsystems are set as 1, i.e. there is no subjective inclination among the subsystems.

Design results of the LAPCAT scenario with different gross take-off weights are shown in Fig. IV-B. The figure indicates that the technical merits and performances of the subsystems decline with weight. The technical merits of the subsystems are plotted in Fig. IV-B.(a). Among the subsystems, when weight is higher than 420 t ($\mu_P \leq 0.1429$), propulsion is the principal subsystem where most technical merit should be paid. When weight is lighter than 420 t, structure becomes the principal. The performances of structure, aerodynamics, and propulsion are respectively plotted in Fig.IV-B.(b), (c), and (d). For a weight lighter than 1200 t ($\mu_P \geq 0.05$), the structural performance exceeds its demonstrated maximum; for one lighter than 1050 t ($\mu_P \geq 0.0571$), the aerodynamic does; for one lighter than 280 t ($\mu_P \geq 0.2143$), the propulsive does. Therefore, advanced technologies of aerodynamics and structure are urgently desired to break through the currently demonstrated levels.

V. CONCLUSION

To enhance the feasibility/accessibility of a hypersonic cruise vehicles (HCV) scenario, a lowest-technical-merit design methodology has been proposed. The methodology could allocate performances/improvements among subsystems, and converge to the most feasible system design scenario. Structure, aerodynamics, and propulsion are involved in construction of the system performance driver, payload/range performance. A hydrocarbon-fueled long-range cruiser has been derived from Boeing X-51A, and a hydrogen-fueled LAPCAT scenario from PREPHA. The simulation results

show that LTM could achieve the optimal allocations while satisfying different payload/range performances. The next works will contain more accurate modelings of the subsystems for hypersonic cruise vehicles. Besides, a payload/range performance driver of periodic cruise is also in consideration.

The remarkable conclusions for the two LTM design cases are detailed as follows:

(1) For hydrocarbon-fueled HCV with different ranges, aerodynamics or structure is the principal subsystem worthing most technical merit.

(2) For hydrogen-fueled HCV with different gross weights (or payload capacities), propulsion or structure is the principal subsystem worthing most technical merit.

(3) In hydrocarbon-/hydrogen-fueled HCV, advanced technologies of structure and aerodynamics are urgently demanded to break through the currently demonstrated levels.

REFERENCES

[1] J. Steelant, R. Varvill, C. Walton, S. Defoort, K. Hannemann, and M. Marini, "Achievements obtained for sustained hypersonic flight within the LAPCAT-II project," in *Proc. 20th AIAA Int. Space Planes Hypersonic Syst. Technol. Conf.*, Glasgow, Scotland, Jul. 2015, p. 3677.

[2] N. Favaloro, G. Pezzella, V. Carandente, R. Scigliano, M. Cicala, and G. Morani, "Design analysis of the high-speed experimental flight test vehicle hexafly-international," in *Proc. 20th AIAA Int. Space Planes Hypersonic Syst. Technol. Conf.*, 2015, p. 3607.

[3] V. Wartemann, A. Wagner, and T. Eggers, "Passive hypersonic boundary layer control: The potential of an ultrasonically absorptive ceramic for HEXAFLY-INT," in *Proc. AIAA AVIATION Forum. Amer. Inst. Aeronaut. Astronaut.*, Jun. 2016, p. 4250. doi: 10.2514/6.2016-4250.

[4] S. Walker, M. Tang, S. Morris, and C. Mamplata, "Falcon HTV-3X—A reusable hypersonic test bed," in *Proc. 15th AIAA Int. Space Planes Hypersonic Syst. Technol. Conf.*, Dayton, OH, USA, Apr. 2008, p. 2544.

[5] Z. Zhang, P. Liu, F. Qin, L. Shi, Y. Wang, and C. Huo, "Numerical and experimental investigation on the influence of inlet contraction ratio for a rocket-based combined cycle engine," *Acta Astron.*, vol. 149, pp. 1–10, Aug. 2018. [Online]. Available: http://www.sciencedirect.com/science/article/pii/S009457651830599X

[6] S. Aso, Y. Tani, and T. Hirayama, "Feasibility study on shared design of hypersonic transport and booster of TSTO for reduction of development cost," in *Proc. AIAA SciTech Forum Amer. Inst. Aeronaut. Astronaut.*, Jan. 2018, p. 0278. doi: 10.2514/6.2018-0278.

[7] E. H. Hirschel and C. Weiland, *Selected Aerothermodynamic Design Problems of Hypersonic Flight Vehicles*. Berlin, Germany: Springer-Verlag, 2009.

[8] J. Chang, R. Zheng, L. Wang, W. Bao, and D. Yu, "Backpressure unstart detection for a scramjet inlet based on information fusion," *Acta Astron.*, vol. 95, pp. 1–14, Feb./Mar. 2014.

[9] S.-K. Im and H. Do, "Unstart phenomena induced by flow choking in scramjet inlet-isolators," *Prog. Aerosp. Sci.*, vol. 97, pp. 1–21, Feb. 2018. [Online]. Available: http://www.sciencedirect.com/science/article/pii/S0376042117301380

[10] P. E. Rodi, S. Emami, and C. A. Trexler, "Unsteady pressure behavior in a ramjet/scramjet inlet," *J. Propuls. Power*, vol. 12, no. 3, pp. 486–493, 1996.

[11] Q. Liu, D. Baccarella, T. Lee, S. Hammack, C. D. Carter, and H. Do, "Influences of inlet geometry modification on scramjet flow and combustion dynamics," *J. Propuls. Power*, vol. 33, no. 5, pp. 1–8, 2017.

[12] J. Zuo, S. Zhang, J. Qin, W. Bao, and N. Cui, "Performance evaluation of regenerative cooling/film cooling for hydrocarbon fueled scramjet engine," *Acta Astron.*, vol. 148, pp. 57–68, Jul. 2018. [Online]. Available: http://www.sciencedirect.com/science/article/pii/S0094576518300171

[13] D. Lou, H. Yan, and J. Zeng, "Flight trajectory optimization for TBCC engine thermal management system design," in *Proc. Int. Space Planes Hypersonic Syst. Technol. Conf.*, Mar. 2017, p. 2293. doi: 10.2514/6.2017-2293.

[14] G. E. Dorrington, "Propulsive efficiency of hypersonic external burning," *J. Spacecraft Rockets*, vol. 37, no. 1, pp. 144–147, Jan. 2000. doi: 10.2514/2.3540.

[15] F. Ding, J. Liu, C.-B. Shen, W. Huang, Z. Liu, and S.-H. Chen, "An overview of waverider design concept in airframe/inlet integration methodology for air-breathing hypersonic vehicles," *Acta Astron.*, vol. 152, pp. 639–656, Nov. 2018.

[16] S. Mölder and E. Timofeev, "Hypersonic air intake design for high performance and starting," Dept. Mech. Eng., McGill Univ., Montreal, PQ, Canada, Tech. Rep. RTO-EN-AVT-195, 2011.

[17] S. H. Miri, "Shock-less hypersonic intakes," M.S. thesis, Ryerson Univ., Toronto, ON, Canada, 2012, Paper 1361.

[18] G. Emanuel, *Gasdynamics: Theory and Applications*. Reston, VA, USA: AIAA, 1986.

[19] P. Dong, H. Tang, and M. Chen, "Study on multi-cycle coupling mechanism of hypersonic precooled combined cycle engine," *Appl. Therm. Eng.*, vol. 131, pp. 497–506, Feb. 2018.

[20] D. Zhang, S. Tang, and J. Che, "Concurrent subspace design optimization and analysis of hypersonic vehicles based on response surface models," *Aerosp. Sci. Technol.*, vol. 42, pp. 39–49, Apr./May 2015.

[21] K. Yuceil, A. Valdivia, J. Wagner, N. Clemens, and D. Dolling, "Active control of supersonic inlet unstart using vortex generator jets," in *Proc. 39th AIAA Fluid Dyn. Conf.*, San Antonio, TX, USA, 2009, p. 4022.

[22] J. D. J. Anderson and G. N. Absi, *Introduction to Flight*, 7th ed. Boston, MA, USA: McGraw-Hill, 2011.

[23] K. G. Bowcutt, "Optimization of hypersonic waveriders derived from cone flows—Including viscous effects," Ph.D. dissertation, Dept. Aerosp. Eng., Univ. Maryland, College Park, MA, USA, 1986.

[24] F. Ding, J. Liu, C.-B. Shen, Z. Liu, S.-H. Chen, and X. Fu, "An overview of research on waverider design methodology," *Acta Astron.*, vol. 140, pp. 190–205, Nov. 2017. [Online]. Available: http://www.sciencedirect.com/science/article/pii/S0094576517309013

[25] F. Deng, F. Xie, N. Qin, W. Huang, L. Wang, and H. Chu, "Drag reduction investigation for hypersonic lifting-body vehicles with aerospike and long penetration mode counterflowing jet," *Aerosp. Sci. Technol.*, vol. 76, pp. 361–373, May 2018.

[26] W. Huang, J. Liu, and Z.-X. Xia, "Drag reduction mechanism induced by a combinational opposing jet and spike concept in supersonic flows," *Acta Astron.*, vol. 115, pp. 24–31, Oct./Nov. 2015. [Online]. Available: http://www.sciencedirect.com/science/article/pii/S0094576515001812

[27] W. Huang, L.-Q. Li, L. Yan, and T.-T. Zhang, "Drag and heat flux reduction mechanism of blunted cone with aerodisks," *Acta Astron.*, vol. 138, pp. 168–175, Sep. 2017. [Online]. Available: http://www.sciencedirect.com/science/article/pii/S0094576517304320

[28] L. Zhu, X. Chen, Y. Li, O. Musa, and C. Zhou, "Investigation of drag and heat reduction induced by a novel combinational lateral jet and spike concept in supersonic flows based on conjugate heat transfer approach," *Acta Astron.*, vol. 142, pp. 300–313, Jan. 2018. [Online]. Available: http://www.sciencedirect.com/science/article/pii/S0094576517311608

[29] E. C. Cockrell, Jr., L. D. Huebner, and D. B. Finley, "Aerodynamic performance and flow-field characteristics of two waverider-derived hypersonic cruise configurations," in *Proc. 33rd Aerosp. Sci. Meeting Exhibit*, Reno, NV, USA, 1995, p. 0736.

[30] M. J. Lewis, "Significance of fuel selection for hypersonic vehicle range," *J. Propuls. Power*, vol. 17, no. 6, pp. 1214–1221, 2001.

[31] L. Jianxia, "Study on the aerodynamic and aero-heating basic problems of hypersonic nonuniform blunt waverider," Ph.D. dissertation, College Aerosp. Sci. Eng., Nat. Univ. Defense Technol., Changsha, China, 2013.

[32] S. Eyi and M. Yumuşak, "Aerothermodynamic shape optimization of hypersonic blunt bodies," *Eng. Optim.*, vol. 47, no. 7, pp. 909–926, 2015. doi: 10.1080/0305215X.2014.933822.

[33] S. Li, Z. Wang, W. Huang, S. Xu, and L. Yan, "Aerodynamic performance investigation on waverider with variable blunt radius in hypersonic flows," *Acta Astron.*, vol. 137, pp. 362–372, Aug. 2017. [Online]. Available: http://www.sciencedirect.com/science/article/pii/S0094576517302734

[34] D. Glass, "Ceramic matrix composite (CMC) thermal protection systems (TPS) and hot structures for hypersonic vehicles," in *Proc. 15th AIAA Int. Space Planes Hypersonic Syst. Technol. Conf.*, 2008, p. 2682.

[35] T.-T. Zhang, Z.-G. Wang, W. Huang, and L. Yan, "A review of parametric approaches specific to aerodynamic design process," *Acta Astron.*, vol. 145, pp. 319–331, Apr. 2018. [Online]. Available: http://www.sciencedirect.com/science/article/pii/S0094576517319045

[36] F. Qu, D. Sun, and G. Zuo, "A study of upwind schemes on the laminar hypersonic heating predictions for the reusable space vehicle," *Acta Astron.*, vol. 147, pp. 412–420, Jun. 2018. [Online]. Available: http://www.sciencedirect.com/science/article/pii/S0094576517316132
[37] J. Steelant, "LAPCAT: High-speed propulsion technology," *Adv. Propuls. Technol.*, vol. 12, no. 1, pp. 1–38, 2008.
[38] L. Serre and S. Defoort, "LAPCAT II: Towards a Mach 8 civil aircraft concept, using advanced rocket/dual-mode ramjet propulsion system," in *Proc. 16th AIAA/DLR/DGLR Int. Space Planes Hypersonic Syst. Technol. Conf.*, 2009, p. 7328.
[39] S. Sharifzadeh, P. Hendrick, S. D'Mello, D. Verstraete, and F. Thirifay, "Structural design optimisation and aerothermoelastic analysis of LAPCAT A2 mach 5 cruise vehicle," in *Proc. 14th AIAA Aviation Technol., Integr., Oper. Conf.*, Atlanta, GA, USA, 2014, p. 2294.
[40] W. B. Scott, "Airbreathing hypersoar would'bounce' on upper atmosphere," *Aviation Week Space Technol.*, vol. 149, no. 10, p. 126, 1998.
[41] M. Sippel, J. Klevanski, and J. Steelant, "Comparative study on options for high-speed intercontinental passenger transports: Air-breathing- vs. rocket-propelled," in *Proc. 56th Int. Astron. Congr. Int. Astron. Fed., Int. Acad. Astronaut., Int. Inst. Space Law*, Fukuoka, Japan, 2005, pp. 1–12. doi: 10.2514/6.IAC-05-D2.4.09.
[42] T. A. Heppenheimer, *Facing the Heat Barrier: A History of Hypersonics*, 1st ed. Washington, DC, USA: NASA, 2007, pp. 2007–4232.
[43] G. J. Harloff and B. M. Berkowitz, "HASA: Hypersonic aerospace sizing analysis for the preliminary design of aerospace vehicles," Sverdrup Technology, NASA Lewis Res. Center Group, Washington, DC, USA, Tech. Rep. 182226, Nov. 1988.
[44] J. M. Hank, J. S. Murphy, and R. C. Mutzman, "The X-51A scramjet engine flight demonstration program," in *Proc. 15th AIAA Int. Space Planes Hypersonic Syst. Technol. Conf.*, Dayton, OH, USA, 2008, p. 2540.
[45] K. J. Murphy, R. J. Nowak, R. A. Thompson, B. R. Hollis, and R. Prabhu, "X-33 hypersonic aerodynamic characteristics," *J. Spacecraft Rockets*, vol. 38, no. 5, pp. 670–683, 2001.
[46] R. Mutzman and S. Murphy, "X-51 development: A chief engineering's perspective," in *Proc. 17th AIAA Int. Space Planes Hypersonic Syst. Technol. Conf.*, Reston, VA, USA, vol. 13, 2011, p. 0846.
[47] W. C. Engelund, S. D. Holland, C. E. Cockrell, Jr., and R. D. Bittner, "Aerodynamic database development for the hyper-X airframe-integrated scramjet propulsion experiments," *J. Spacecraft Rockets*, vol. 38, no. 6, pp. 803–810, Nov. 2001. doi: 10.2514/2.3768.
[48] L. J. Williams, "Estimated aerodynamics of all-body hypersonic aircraft configurations," Office Adv. Res. Technol. Mission Anal. Division, Moffett Field, Mountain View, CA, USA, Tech. Rep. NASA TM X-2091, 1971.
[49] G. J. Harloff, "High angle-of-attack hypersonic aerodynamics," *J. Spacecraft Rockets*, vol. 25, no. 5, pp. 343–344, 1988.
[50] F. Ding, J. Liu, C.-B. Shen, and W. Huang, "Novel approach for design of a waverider vehicle generated from axisymmetric supersonic flows past a pointed von karman ogive," *Aerosp. Sci. Technol.*, vol. 42, pp. 297–308, Apr. 2015.
[51] C. Wang, X. Tian, L. Yan, L. Xue, and K. Cheng, "Preliminary integrated design of hypersonic vehicle configurations including inward-turning inlets," *J. Aerosp. Eng.*, vol. 28, no. 6, 2014, Art. no. 04014143.
[52] Z. Huiyu, W. Gang, S. Quanhua, and F. Jing, "Numerical evaluation on areodynamics of typical hypersonic configurations for hypersonic flight," *Acta Aerodyn. Sinica*, vol. 30, no. 3, pp. 365–372, 2012.
[53] W. H. Heiser and D. T. Pratt, *Hypersonic Airbreathing Propulsion*. Washington, DC, USA: AIAA Education Series, 1994.
[54] A. L. Kuranov, A. V. Korabelnicov, V. V. Kuchinsky, and E. G. Sheikin, "Modern condition of development and perspective researches of hypersonic technologies under the 'AJAX' concept," in *Proc. 2nd Workshop Magneto-Plasma-Aerodyn. Aerosp. Appl.*, Moscow, Russia, 2000, pp. 15–21.

WENKAI WANG received the B.Sc. degree in space engineering and the M.Sc. degree in aeronautical and astronautical science and technology from the National University of Defence Technology (NUDT), China, in 2012 and 2014, respectively, where he is currently pursuing the Ph.D. degree in aeronautical and astronautical science and technology under the supervision of Prof. Z. Hou with the College of Aerospace Science and Engineering. He has authored or coauthored several articles in the field of aircraft design and control. His current research interests include preliminary design, flight dynamics, and optimal control for hypersonic cruise vehicles.

ZHONGXI HOU received the Ph.D. degree in computational fluid dynamics from the National University of Defence Technology (NUDT), China, in 2000. He is currently a Professor in aeronautical and astronautical science and technology. He founded the Near Space Technology Research Center, NUDT. He has authored a monograph and over 40 international journals. His main research interests include aircraft conceptual design technology of high-altitude long-endurance (HALE) solar-powered unmanned aircraft systems (UAS), the aerodynamics parameters study of aircrafts, high resolution and high efficient computational methods in CFD, parallel calculated methods on cluster of workstations (COWs) and massively parallel processing (MPP) systems with message passing interface (MPI) service.

XIANZHONG GAO received the B.Sc. degree in space engineering and the M.Sc. and Ph.D. degrees in aeronautical and astronautical science and technology from the National University of Defence Technology (NUDT), Changsha, China, in 2007, 2009, and 2014, respectively, where he is currently a Lecturer. His research interests include the general design of nearspace vehicle, and the application of machine learning in nearspace vehicle and UAVs.

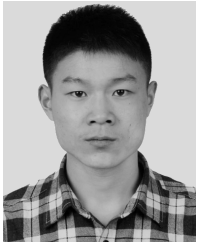

LILI CHEN received the B.Sc. degree in space engineering and the M.Sc. degree in aeronautical and astronautical science and technology from the National University of Defence Technology (NUDT), China, in 2013 and 2015, respectively, where he is currently pursuing the Ph.D. degree in aeronautical and astronautical science and technology under the supervision of Prof. Z. Guo with the College of Aerospace Science and Engineering. He has authored or coauthored several articles in the field of aerodynamic design and CFD. His current research interest includes aerodynamic design for hypersonic cruise vehicles.